

Primljen / Received: 7.12.2018.
 Ispravljen / Corrected: 3.3.2019.
 Prihvaćen / Accepted: 11.3.2019.
 Dostupno online / Available online: 10.7.2019.

Bending moment curvature relationship as an indicator of seismic resistance of older bridge piers

Authors:



Mladen Srbić, PhD. CE
 University of Zagreb
 Faculty of Civil Engineering
msrbic@grad.hr

Preliminary note

Mladen Srbić, Ana Mandić Ivanković, Tomislav Brozović

Bending moment curvature relationship as an indicator of seismic resistance of older bridge piers

In seismic areas, it is recommended to design bridges characterized by ductile behaviour. A large number of existing bridges designed according to outdated standards, without guidelines for ductile behaviour detailing, can be found in seismically active areas. The level of ductility exhibited by these bridges is unknown. A crucial seismic performance indicator for older bridges with piers containing smooth reinforcing bars, i.e. the bending moment-curvature curve ($M-\phi$ curve), is considered in this paper. The results of analytical, experimental and numerical approaches for determining the $M-\phi$ curve are compared, and conclusions on the effect of smooth reinforcement slippage are presented.

Key words:

seismic resistance, old bridge, bending moment, curvature, smooth reinforcement

Prethodno priopćenje

Mladen Srbić, Ana Mandić Ivanković, Tomislav Brozović

Odnos momenta savijanja i zakrivljenosti kao pokazatelj seizmičke otpornosti stupova starijih mostova

U seizmički aktivnim područjima poželjno je projektirati mostove duktilnog ponašanja. Veliki se broj postojećih mostova, projektiranih prema danas zastarjelim normama, a koje nisu nudile smjernice za oblikovanje elemenata za duktilno ponašanje, nalaze se u seizmički aktivnim područjima. Nepoznata je razina duktilnosti koju ti mostovi posjeduju. U ovome se radu razmatra jedan od bitnih pokazatelja seizmičke otpornosti starijih mostova sa stupovima u kojima je ugrađena glatka armatura – krivulja ovisnosti momenta savijanja i zakrivljenosti, $M-\phi$ krivulja. Uspoređeni su rezultati analitičkog, eksperimentalnog i numeričkog pristupa u određivanju krivulje te su doneseni zaključci o utjecaju proklizavanja glatke armature.

Ključne riječi:

seizmička otpornost, stari most, moment savijanja, zakrivljenost, glatka armatura

Vorherige Mitteilung

Mladen Srbić, Ana Mandić Ivanković, Tomislav Brozović

Das Verhältnis von Biege- und Krümmungsmoment als Indikator für den seismischen Widerstand der Säulen älterer Brücken

In seismisch aktiven Gebieten ist es wünschenswert, Brücken mit duktilem Verhalten zu konstruieren. In seismisch aktiven Gebieten befindet sich eine große Anzahl vorhandener Brücken, die nach den heute veralteten Normen konstruiert wurden und keine Richtlinien für die Bildung von Elementen für duktile Verhalten boten. Der Grad der Duktilität dieser Brücken ist unbekannt. In dieser Arbeit wird ein wichtiger Indikator für den seismischen Widerstand älterer Brücken mit Pfeilern, in die eine glatte Bewehrung eingebaut wurde, betrachtet – die Kurve der Abhängigkeit des Biege- und Krümmungsmoments, $M-\phi$ -Kurve. Die Ergebnisse des analytischen, experimentellen und numerischen Ansatzes zur Bestimmung der Kurve wurden verglichen und Rückschlüsse auf den Einfluss des Abrutschens der glatten Bewehrung gezogen.

Schlüsselwörter:

seismischer Widerstand, alte Brücke, Biegemoment, Krümmung, glatte Bewehrung

1. Introduction

As the entire Croatian territory is located in a seismically active area, earthquakes are often adopted as main load when dimensioning bridge elements (columns in particular), and when defining material consumption, solving details, and determining overall mechanical resistance and stability of bridges. A review of literature relating to the field of seismic resistance reveals that most of the research has been focusing on the calculation and design of new bridges or buildings [1-5]. The existing bridge structures, often designed according to former seismic regulations, or even devoid of any seismic design, may still contain reserves of seismic resistance that should be detected using appropriate assessment methods [6, 7] and suitable seismic performance indicators [8-10].

The seismic resistance of bridges is affected by a number of parameters. One of major properties that structures must possess in seismically active areas is the nonlinear response or ductile behaviour [11]. This property will largely depend on the properties of construction materials, and on the design and solution of structural details. When assessing seismic resistance, the main unknown is the level of ductility exhibited by the structure, or the level of seismic force that can be absorbed through formation of plastic hinges and deformability in the zone of nonlinear behaviour. Currently, the knowledge is still insufficient about the ductility levels of columns of non-standard cross-section, designed without heed to ductile behaviour, and about development of plastic hinges and, more broadly, about non-linear behaviour of such structures. Investigating performance of columns characterized by such cross-sections could lead to improvement of methods currently used for evaluation of bridges in seismically active areas.

One of key indicators of seismic capacity of bridge columns is the moment curvature relationship, $M-\varphi$ curve, which best illustrates the rotational capacity of plastic hinges [12-16]. The determination of the $M-\varphi$ curve of a column model based on a real column from the Šibenik Bridge is presented in the paper, and this through:

- analytical calculation based on the developed parametric algorithm
- laboratory testing
- numerical analysis using a typical bridge-modelling software.

Because of the polygonal cross section and use of smooth reinforcement, the Šibenik Bridge constitutes an appropriate case study for this research. The moment curvature relationship results were compared in order to determine specific effects of smooth reinforcement [17] on the seismic capacity of bridge elements, and to assess suitability of the most common calculation models.

2. Moment curvature relationship

The seismic resistance of existing bridges can only be assessed by means of an appropriate nonlinear method. However, the

application of nonlinear methods requires knowledge of real behaviour of structural elements, i.e. the rotational capacity of elements ($M-\varphi$ diagrams) under static load in the case of a nonlinear static analysis, or cyclic load in the case of a nonlinear dynamic analysis.

When calculating the moment curvature relationship of the cross section, the diagram can be displayed in two ways: a) as the bi-linear diagram [5] - a dashed polygonal curve shown in Figure 1 which does not reveal the state until the first crack and b) as the three-linear diagram [18] - the red polygonal curve shown in Figure 1 approximated through three characteristic points as boundaries of three domains through which the cross-section passes during increase in load.

The first domain is characterized by the elasticity of cross section: stresses observed at each point of the cross section are lower than the tensile strength of concrete, and the cross section has not yet cracked. The second domain is characterized by the cross section after occurrence of first crack and until the yield of tensile reinforcement. After the first crack occurs in concrete, the height of the concrete section is reduced and compressive stresses in concrete are now transferred via the remaining concrete areas and compression reinforcement, while the tensile stress is transferred via the tensile reinforcement only. After the yield of tensile reinforcement, the cross section is in the third domain until the final collapse of the structure. The collapse of the structure can occur via the reinforcement or concrete. The relevant value is the one in which the failure occurred first.

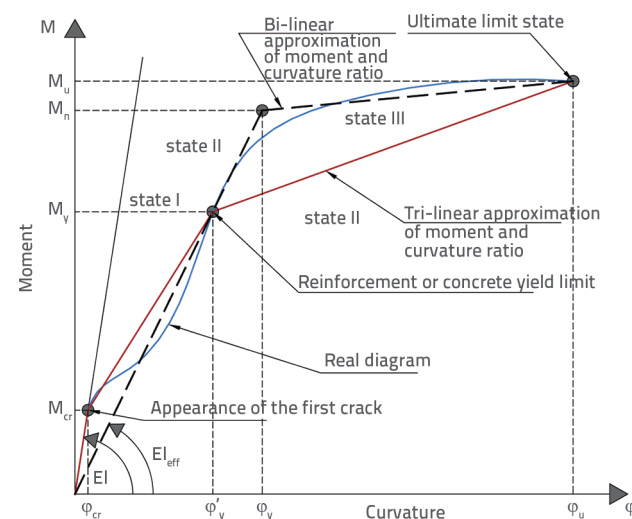


Figure 1. Typical layout of $M-\varphi$ diagrams

However, when detecting potential hidden reserves, only the real curve of the moment curvature relationship of the reinforced-concrete cross section (blue curve in Figure 1), which significantly deviates from idealized curves, presents a reliable indicator of the bearing capacity of elements exposed to seismic

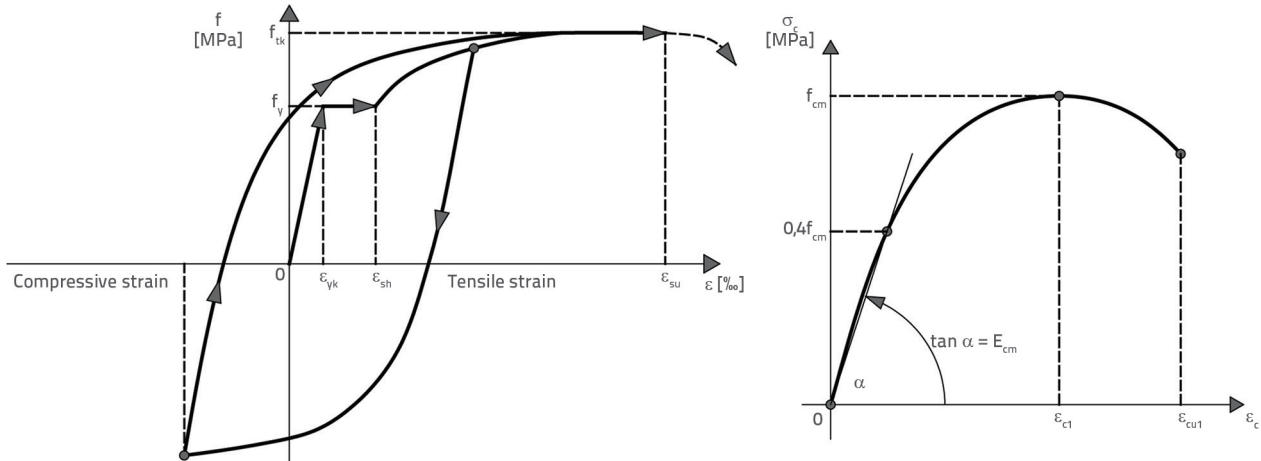


Figure 2. Stress and strain relationship applied in calculation of $M-\varphi$ diagram, left: for reinforcement, right: for concrete

action [12, 14]. The impact of crack propagation on the moment curvature relationship of cross section, after the tensile strength of concrete has been reached, is shown in [13].

In Figure 1, M_N is the nominal bending moment resistance, φ_y is the curvature at yield of the equivalent bi-linear approximation of the moment curvature ratio, M_{cr} is the bending moment, and φ_{cr} is the curvature of cross section at first crack, M_y is the bending moment at yield limit, φ'_y is the curvature of cross section at yield limit of concrete or reinforcement, M_u is the bending moment, and φ_u is the curvature at ultimate bearing capacity. In the following section, the $M-\varphi$ curve is analysed:

- by analytical method via parametric analysis
- experimentally based on laboratory testing of column model
- numerically using an appropriate software.

2.1. Analytical method

Taking into consideration the algorithm defined in [14] for a hollow rectangular section, an algorithm was developed in this study for analytical calculation of $M-\varphi$ properties of non-typical nonlinear polygonal column cross sections with real properties of smooth reinforcement (based on the Šibenik bridge columns) through three characteristic points: point in which the concrete tensile strength is reached at the tensile edge of cross-section immediately before formation of first crack, reinforcement yield point and point in which the ultimate limit state is reached via concrete or reinforcement failure.

Each of the above-mentioned points is characterized by the known size of relative deformation at the corresponding part of cross-section (relative deformation when the tensile strength of concrete is reached, yield limit of concrete or reinforcement, and ultimate limit state of concrete or reinforcement). Assuming Bernoulli's hypothesis and knowledge of relative deformation of cross section at one point, we are looking for curvature in which cross-section forces will be in balance. This is an iterative procedure in which the cross-section curvature must be changed until the state of balance is achieved. The cross-section resistance

moment is determined from the known cross-sectional balance forces for a characteristic point. The values between individual points of the moment curvature diagram are obtained by increasing relative deformation of the characteristic part of cross section, from the value corresponding to the first point, to the value corresponding to the second point of the $M-\varphi$ diagram. Specific features of this algorithm, compared to the ones developed so far, is the adjustment to polygonal cross-section and the introduction of non-linear behaviour of materials. The values of each force are determined from the known values of relative deformation of cross-section and the strain-deformation relationship of each material. The nonlinear distribution of compressive stress and strain values for concrete was developed according to [19], while the nonlinear behaviour of reinforcement was defined according to [5] (Figure 2). The parameters required to define these relationships were obtained by examining properties of the materials used in the column model prepared for experimental testing. The usual approach to the calculation of confined concrete elements is to adopt properties of confined concrete for the concrete part of cross-section within the confinement zone, while properties of unconfined concrete are adopted for the concrete outside of the confinement zone [20]. As the subject of this study are the columns of older bridges for which no seismic design guidelines were used (the columns do not have confined reinforcement in the area of plastic hinges nor the quantity of shear reinforcement sufficient to withstand seismic action), the properties of unconfined concrete were adopted throughout the cross-section in this numerical and analytical analysis.

The force at the part of cross-section with nonlinear distribution of compressive stress is determined by dividing the concrete section into a sufficient number of infinitesimally small surfaces of the corresponding width and height, which are then multiplied with the corresponding stress value at that height (Figure 3). The total force of the compressive area of concrete is the sum of all forces of the infinitesimal division of cross section.

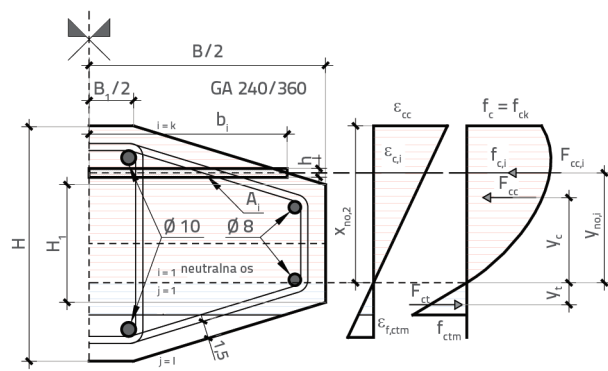


Figure 3. Distribution of compression and tensile areas of concrete for calculation of internal forces

In Figure 3, h_i represents the height of the infinitesimal section, b_i is the width of the infinitesimal section, ε_{cc} is the strain at the compression edge of concrete, ε_{ci} is the strain at the height of an infinitesimal section, ε_{ctm} is the strain when the tensile strength of concrete is reached, f_c is the concrete compression stress at the edge of cross section, f_{ctm} is the tensile strength of concrete, F_{cc} is the resultant force of concrete at the compression part of the section, F_{ct} is the resultant force of concrete at the tensile part of the section, and F_{ccj} is the force at the infinitesimal part of the section.

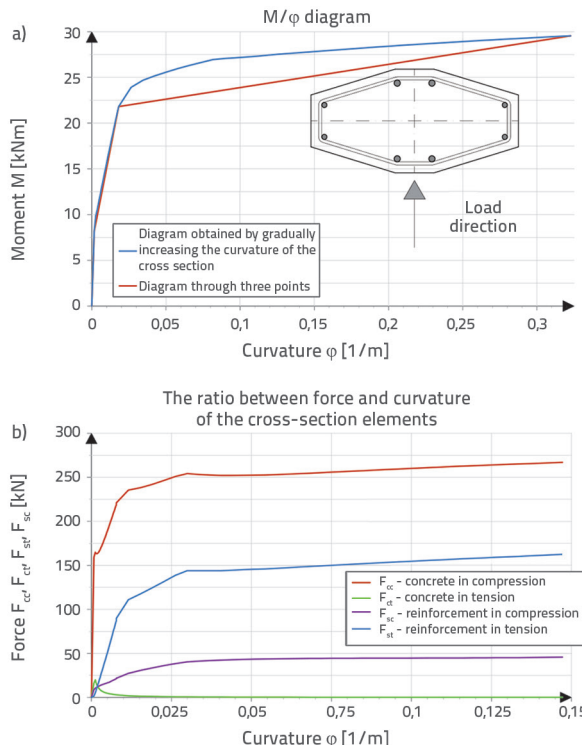


Figure 4. a) M- φ diagram for column obtained by analytical procedure; b) dependence of internal forces on cross-section curvature

The moment-curvature relationship results (M- φ diagram) obtained by the above described procedure are presented below

(Figure 4a). The ultimate limit state of cross section was reached through relative strain of concrete in compression. The results for bending about the lower axis of the column cross section are shown. The values of forces for each cross-sectional element (concrete in compression, concrete in tension, compressive and tensile reinforcement) are presented in Figure 4b together with the M- φ diagram values. The moment curvature ratio presented via three points is more appropriate for engineering practice, while the diagram obtained by gradual increase of curvature based on a greater number of points is more appropriate for scientific research [14]. This diagram covers the above-mentioned three typical points, as well as the area between these points.

2.2. Laboratory testing

A column forming part of a static cantilever system was tested. The column was anchored to an anchoring block fixed to the laboratory floor. Cauchy's relationships [21] were applied for reducing the physical size of the real bridge column (Figure 5) to the size of the column model (Figure 3). Cross sectional dimensions of the column model are shown in Table 1.

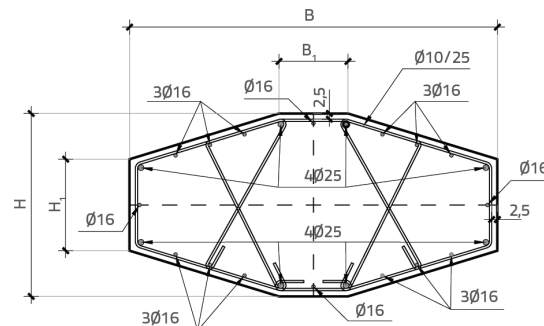


Figure 5. Typical column cross section (Šibenik Bridge)

Table 1. Dimensions and material properties of the column

Parameter / property of the column	Real column	Test model column
Column height h [m]	24	1.84 (6.0)
Cross-sectional width B [cm]	160	40
Cross-sectional height H [cm]	80	20
Straight section width B_1 [cm]	30	7.5
Straight section height H_1 [cm]	40	10
Concrete	MB 450	C35/45
Reinforcement	GA 240/360	GA 240/360
Reinforcement diameter	16Ø16. 8Ø25	4Ø8. 4Ø10
Reinforcement area	$A = 71.44 \text{ cm}^2$	$A = 5.16 \text{ cm}^2$
Percentage of reinforcement	0.7 %	0.8 %

The model testing was carried out at the Laboratory for Materials and Structures of the Institute IGH in Zagreb. The required load level for the column model was determined using the Sofistik software that is traditionally applied in the engineering analysis of structures. The dead load and earthquake action effects were analysed by applying the three dimensional finite element bridge model, using material and geometrical properties from the detailed and working design of the bridge. The modal analysis involving load spectrum typical for the actual bridge site was carried out for the seismic load assessment. The load level for the experimental model was defined based on the final element model analyses for the bridge. The ultimate shear stress at the bottom of the column was avoided by means of an appropriately chosen column height to cross section ratio.

Some column model parameters could not be derived from model similarities. The most significant deviation was in the height chosen for the test model column, and the height obtained from the model similarity. However, the dominant column bending load was ensured by the selected ratio of the column model height to column model cross-sectional height, while the impact of shear was reduced to minimum.



Figure 6. a) Column test set up in laboratory, b) crack opening at column end section

The model conceived in this way, subjected to an adjusted load, is characterized by the end column section behaviour that corresponds to that of the column model whose height is selected based on model similarity.

Thus, a higher column height would result in a smaller transverse force at the top of the column, and in a greater P/Δ impact on the end-section bending moment. The quantity and characteristics of longitudinal reinforcement are also a significant parameter for determining behaviour of the experimental model. It can be expected that the difference in the quantity of longitudinal reinforcement of the tested column model will result in a greater bearing capacity of the model compared to the real column.

The model testing was conducted using two hydraulic jacks, a vertical jack for application of axial force, and a horizontal jack for applying transverse force at the top of the column (Figure 6). The intensity of individual load was measured by load gauges positioned at each jack. The horizontal variable load was introduced by displacement control, while vertical load was constant and involved corrections due to deflection of the top of the column. The axial force value was set to 100 kN. The monotonous horizontal load was introduced with a constant increase of displacement in 10 mm increments, with pauses between each step to read measurement results and check the measuring equipment.

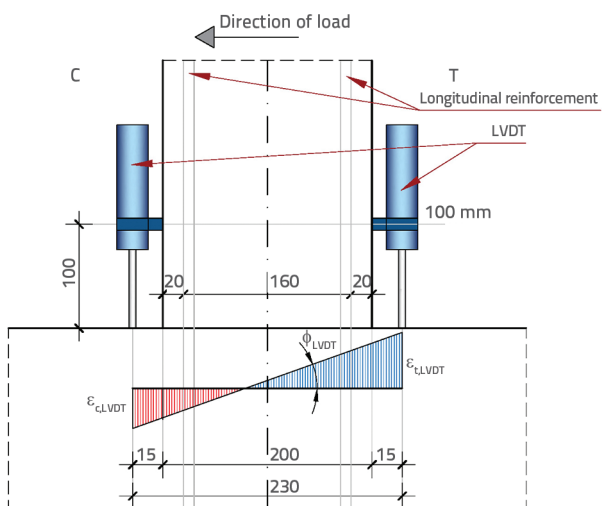


Figure 7. Setup of measuring devices at column bottom to measure rotation of end section

The moment acting on the bottom of the column is the result of three components: horizontal load introduced by horizontal jack, horizontal component of vertical jack load due to column displacement, and the vertical force component due to the $P-\Delta$ effect. These force components were determined by measuring horizontal displacement with a LVDT measuring device positioned at the top of the column. The end section rotation (cross section at the anchor block to column connection, column bottom) was measured with two LVDTs (100 mm measuring base) located at the bottom of the column (Figure 7). The bases of measuring devices were attached to the column (the LVDT

base was 100 mm away from the bottom of the column), while the needle of LVDT devices was attached to the anchor block of the column. The curvature of the end section was determined using relative deformations measured on both sides of the column. The above described setup of measuring devices and definition of loads enabled determination of the bending moment and the end section curvature at any point in time during realisation of the test.

The curve representing experimental relationship between the bending moment and curvature is shown in Figure 8. In addition to measurements required to define the $M-\varphi$ diagram, the relative strain of reinforcement were also measured. The measurement was carried out using the 3 mm measuring base strain gauges, which were placed at the studied end-section of reinforcement prior to concreting. The reinforcement yield limit was determined from the measured relative deformations and based on the known characteristics of the embedded reinforcement. The mark M_y stands for the experimental bending moment at yield point of the reinforcement. It is represented with a rhomb within the diagram in Figure 8. The dominant rotation of the end section, and the ultimate concrete related limit state, were observed after the experimental model testing. This corresponds to results obtained by analytical calculation.

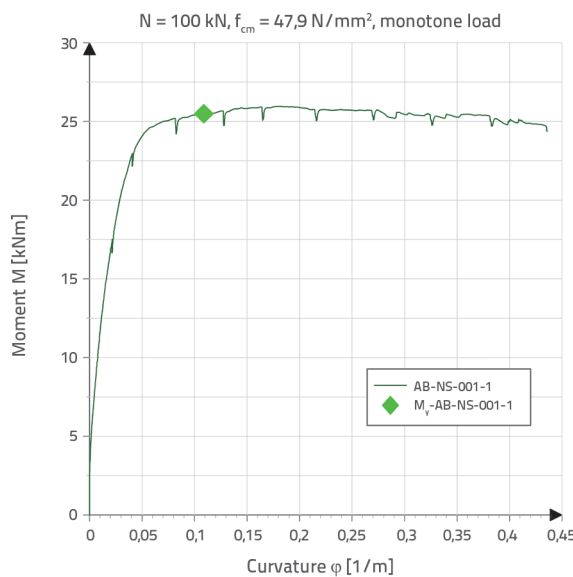


Figure 8. $M-\varphi$ curve obtained experimentally at the test model of the column

2.3. Numerical analysis

The numerical analysis of experimentally tested columns was carried out by means of the Sofistik software, using a nonlinear calculation, including material and geometrical nonlinearity. The numerical model of the column was also adapted to the laboratory-tested column in terms of cross-sectional dimensions, reinforcement distribution, and material properties. Horizontal and vertical loads were applied at the top of the column. The full vertical load was immediately applied

and it remained unchanged until the end of the calculation. The horizontal load was applied in increments from zero to maximum horizontal force that the numerical model can handle before failure. The results of this part of the study are expressed as numerically derived dependencies of the horizontal force and displacement (AB-NS-001-1), and dependences of the bending moment and curvature of the column cross section (Numerical-AB-NS-001-1), as presented at Figure 9.

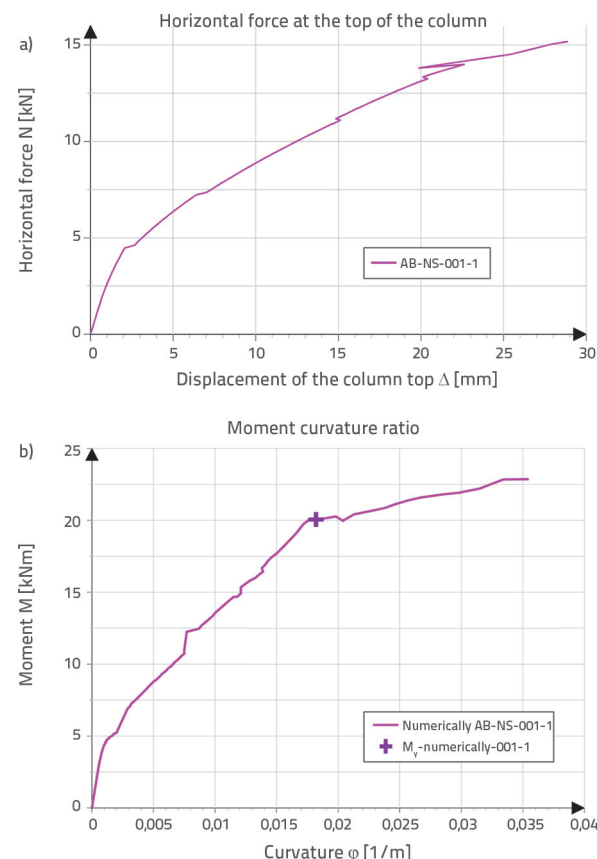


Figure 9. a) Numerically obtained $P-\Delta$ and b) $M-\varphi$ curve for column model subjected to testing

The mark M_y stands for the numerical bending moment when the yield point of reinforcement is reached. It is represented by cross mark in the diagram shown in Figure 9.

3. Comparison of results with conclusions

A comparison of results obtained by the three above described procedures is presented in Figure 10. The bending moment - curvature relationship curves show very good matching in the linear range, while significant deviation of experimental results from the analytical and numerical ones can be observed after the numerical (pink cross mark) or analytical (blue triangle mark) yield point, and further in the area of nonlinear behaviour. The difference in the cross-section curvature when reaching the yield limit is shown with $\Delta\varphi_y$ in Figure 10 for analytical and numerical calculations, as related to the cross-section curvature obtained experimentally.

The experimental analysis shows the representative relationship between the bending moment and curvature and the relative reinforcement deformation in the end section (maximum torque section), at any time point during the testing. The experimentally obtained relationship (curve marked with green in Figure 10) consists of two characteristic parts: elastic part (matching the analytically obtained blue and numerically obtained pink curve) and plastic part (almost horizontal part of the green curve). According to Figure 1, the theoretical yield point of reinforcement is at a point where the moment-curvature relationship starts to deviate from the elastic part, and moves towards the plastic part. On the experimentally obtained curve, this point should be close to the analytically and numerically obtained yield limit of the reinforcement (blue triangle and pink cross). By measuring relative deformation of reinforcement at the maximally loaded cross section, it was established that the experimental yield point (green rhomb in Figure 10) corresponds to the significantly larger curvature value as compared to the theoretical yield point.

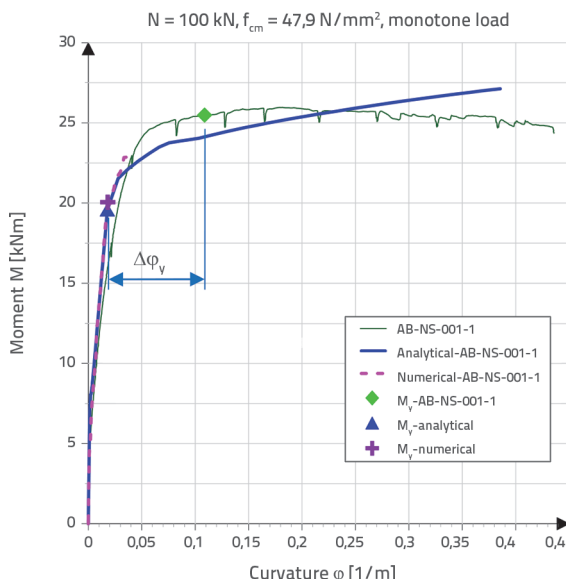


Figure 10. Comparison of analytically, numerically and experimentally obtained $M-\varphi$ curve of the column

This deviation is due to the effect of slipping of smooth reinforcement from the anchoring zone below the end section. Namely, the loss of adhesion extends the length of the non-anchored tension reinforcement, which results in greater relative deformation, and thus in greater rotation of the cross section at the maximum moment section. In addition, by comparing experimental and analytical results, it can be seen that the slip effect reduces as the ultimate limit state is approached (the green curve of the experiment remains approximately horizontal, and even decreases, while the blue curve of the analytical procedure slightly increases).

The deviation of the numerically obtained $M-\varphi$ relationship from the values obtained by analytical procedure clearly indicates that the software traditionally used in structural engineering analysis

(software based on the assumption of rigid bond between reinforcement and concrete) should not be applied for assessing hidden reserves of ductility elements. Therefore, when modelling existing structures, it would be advisable to determine properties of actually built-in reinforcement and concrete (in terms of bearing capacity and deformability) and to develop the finite element model for reinforcement and concrete, which would also focus on adhesion between these two materials.

In the light of the above discussion, the use of analytical approach can be recommended for creating the relationship curve between bending moment and curvature of untypical cross sections, provided that corrections be made for elements reinforced with smooth reinforcement that were not realized according to guidelines for ductile behaviour. These corrections could be defined more accurately by considering more extensive research results, as announced in Section 4 of this paper.

4. Further research

The relationships between the bending moment and curvature of nonstandard cross sections with smooth reinforcement, as obtained by

- analytical
- experimental
- numerical methods

are compared in this paper using a bridge column model.

It is considered that the disparity of curvature values at yield limit in individual methods is due to slippage of smooth reinforcement, which confirms the hypothesis that standardised traditional procedures for the determination of seismic resistance indicators – in this case $M-\varphi$ curves representing the relationship between bending moment and curvature of cross-section – can not be applied for assessing seismic resistance of old bridges with smooth reinforcement.

Further research is expected to better define seismic resistance indicators for older bridges. This research will include the following extensive laboratory testing:

- Control testing of mechanical properties of materials (concrete, smooth and ribbed reinforcement of different profiles).
- Testing of bond and slippage of smooth steel reinforcement, using samples of concrete beams with a joint in the middle, according to the procedure defined in the report presented by the International Federation for Structural Concrete [22].
- Calibration and testing of measuring equipment on one column sample.
- Testing seismic resistance indicators (chord rotation capacity, cross section curvature) with monotonous load on seven (7) column samples; six (6) samples reinforced with smooth reinforcement and one (1) reinforced with ribbed reinforcement; at that, the length of plastic hinges will be studied on three (3) samples.
- Testing seismic resistance (chord rotation capacity, cross section curvature) with cyclic load on eight (8) column

samples; seven (7) reinforced with smooth reinforcement and one (1) reinforced with ribbed reinforcement; at that, the length of plastic hinges will be studied on three (3) samples.

Results obtained by experimental research will be compared with analytical and numerical methods. In addition to the relationship of the bending moment and curvature of the end section, which is presented and considered in this paper based on one-column test, further study will cover the bases of all tests. Furthermore, some additional seismic resistance indicators will be compared:

- curvature of end cross section at yield limit
- curvature of end cross section at ultimate limit state
- length of plastic hinges
- chord rotation capacity at yield limit
- chord rotation capacity at ultimate limit state.

In that respect, numerical, analytical and experimental results for different points along the height of the plastic joint will be compared with those to be obtained in accordance with EN 1998-3 [23] and expressions based on latest scientific research [3, 4]. Separate comparisons will be made for monotonous and cyclically loaded samples.

The authors believe that the results of the research will be used to adjust standardized expressions for seismic resistance indicators of the elements reinforced with smooth reinforcement, and to suitably model existing structures in order to cover real-life seismic resistance of older bridge columns. Thus, the results of this research will contribute to the improvement of seismic assessment of the existing bridges that were not designed in accordance with modern guidelines for ductile behaviour, the aim being to ensure an optimum management of the existing infrastructure.

REFERENCES

- [1] Panagiotakos, T.B., Fardis, M.N.: Deformations of Reinforced Concrete Members at Yielding and Ultimate. *ACI Struct J.*, 98 (2001), pp. 135–148.
- [2] Paulay, T., Priestley, N.: Seismic Design of Reinforced Concrete and Masonry Buildings. John Wiley & Sons, Inc. 1992, <https://doi.org/10.1002/9780470172841>
- [3] Biskinis, D., Fardis, M.N.: Deformations at flexural yielding of members with continuous or lap-spliced bars, *Structural Concrete*, 11 (2010) 3, pp. 127-138.
- [4] Biskinis, D., Fardis, M.N.: Flexure-controlled ultimate deformations of members with continuous or lap-spliced bars, *Structural Concrete*, 11 (2010) 2, pp. 93-108.
- [5] Priestley, M.J.N., Calvi, G.M.: Displacement Based Seismic Design of Structures. 2007.
- [6] Franetović, M., Mandić Ivanković, A., Radić, J.: Seismic Assessment of Existing Reinforced Concrete Arch Bridges, *GRAĐEVINAR*, 66 (2014) 8, pp. 691-703, doi: <https://doi.org/10.14256/JCE.1073.2014>
- [7] Paraskeva, T.S., Kappos, A.J.: Further development of a multimodal pushover analysis procedure for seismic assessment of bridges. *Earthquake Engineering and Structural Dynamics*, 39 (2010) 2, pp. 211-222.
- [8] Mandić Ivanković, A., Srbic, M., Radic, J.: Performance indicators in assessment of concrete arch bridges. *Maintenance, Monitoring, Safety, Risk and Resilience of Bridges and Bridge Networks*. Túlio N. Bittencourt; Dan M.Frangopol; André T. Beck (ed.).London, UK: CRC Press /Balkema, IABMAS2016. 301(948)-302(955)
- [9] Mandić Ivanković, A., Srbic, M., Radić, J.: Seismic Performance of Concrete Arch Bridges. *Performance-Based Approaches for Concrete Structures*.Beushausen. Cape Town, South Africa: FIB, 2016, pp. 237-238
- [10] Mandić Ivanković, A., Srbic, M., Franetović, M.: Performance of existing concrete arch bridges. *IABSE Conference 2015 - Structural Engineering: Providing Solutions to Global Challenges*. Geneva, Switzerland, September 23-25, pp. 1033-1040, 2015, <https://doi.org/10.2749/222137815818358268>
- [11] Priestley, M.J.N. Seible, F. Calvi, G.M.: Seismic Design and Retrofit of Bridges. New York: John Wiley & Sons, INC.; 1996, <https://doi.org/10.1002/9780470172858>
- [12] Chandrasekaran, S., Nunziante, L., Serino, G., Carannante, F.: *Seismic Design Aids for Nonlinear Analysis of Reinforced Concrete Structures*, 2009.
- [13] Creazza, G., di Marco, R.: Bending moment-mean curvature relationship with constant axial load in the presence of tension stiffening, *Materials and Structures*, 26 (1993), pp. 196-206, <https://doi.org/10.1007/BF02472612>
- [14] Čurić, I., Radić, J., Franetović, M.: Determination of the Bending Moment – Curvature Relationship for Bridge Concrete Columns, *Teh Vjesn - Tech Gaz.*, 23 (2016) 3, pp. 907-915.
- [15] Priestley, M.J.N.: Myths and Fallacies in Earthquake Engineering. Revisited The Ninth Mallet Milne Lecture, 2003. 2003;98
- [16] Espion, B., Halleux, P.: Moment curvature relationship of RC sections under combined bending and normal force, *Materials and Structures*, 21 (1988), pp. 341-351, <https://doi.org/10.1007/BF02472160>
- [17] Verderame, G.M., Ricci, P., Manfredi, G., Cosenza, E.: Ultimate Chord Rotation of RC Columns with Smooth Bars: Some Considerations about EC8 Prescriptions, *Bulletin of Earthquake Engineering*, 8 (2010) 6, pp. 1351-1373.
- [18] Baker, A.L.L.: *Ultimate Load Design of Reinforced Concrete Frames: A Recapitulation and Appraisal*, IABSE Publ. 1963
- [19] Eurocode: *Eurocode 2 - Design of Concrete Structures - Part 1-1: General Rules and Rules for Buildings*. Vol. BS En 1992. Brussels: European Committee for Standardization CEN, 2004. BS En 1992 225 p. (vol. BS En 1992).
- [20] Mander, B.J., Priestley, J.N.M., Park, R.: Theoretical stress-strain model for confined concrete, *ASCE, Struct. J.*, 144 (1988) 8, pp. 1804-1826.
- [21] Taucer, F., Pinto, A.V.: Mock-up Design of Reinforced Concrete Bridge Piers for PsD Testing at the ELSA Laboratory : (Vulnerability Assessment of Bridges Project), 2000.
- [22] Fib bulletin 10, Bond of reinforcement in concrete, August 2000
- [23] Eurocode. *Eurocode 8: Design of Structures for Earthquake Resistance - Part 3 - Assessment and Retrofitting of Buildings*. Vol. 3. Brussels: European Committee for Standardization CEN; 2004.3. (vol. 3).